



ARTICLE

An Advanced Bald Eagle Search Algorithm for Image Enhancement

Pei Hu¹, Yibo Han¹ and Jeng-Shyang Pan^{2,3,*}

¹School of Computer and Software, Nanyang Institute of Technology, Nanyang, 473004, China

²College of Artificial Intelligence, Nanjing University of Information Science and Technology, Nanjing, 210044, China

³Department of Information Management, Chaoyang University of Technology, Taichung, 413310, Taiwan

* Corresponding Author: Jeng-Shyang Pan. Email: jengshyangpan@gmail.com

Received: 16 October 2024; Accepted: 11 December 2024; Published: 06 March 2025

ABSTRACT: Image enhancement utilizes intensity transformation functions to maximize the information content of enhanced images. This paper approaches the topic as an optimization problem and uses the bald eagle search (BES) algorithm to achieve optimal results. In our proposed model, gamma correction and Retinex address color cast issues and enhance image edges and details. The final enhanced image is obtained through color balancing. The BES algorithm seeks the optimal solution through the selection, search, and swooping stages. However, it is prone to getting stuck in local optima and converges slowly. To overcome these limitations, we propose an improved BES algorithm (ABES) with enhanced population learning, position updates, and control parameters. ABES is employed to optimize the core parameters of gamma correction and Retinex to improve image quality, and the maximization of information entropy is utilized as the objective function. Real benchmark images are collected to validate its performance. Experimental results demonstrate that ABES outperforms the existing image enhancement methods, including the flower pollination algorithm, the chimp optimization algorithm, particle swarm optimization, and BES, in terms of information entropy, peak signal-to-noise ratio (PSNR), structural similarity index (SSIM), and patch-based contrast quality index (PCQI). ABES demonstrates superior performance both qualitatively and quantitatively, and it helps enhance prominent features and contrast in the images while maintaining the natural appearance of the original images.

KEYWORDS: Image enhancement; gamma correction; retinex; bald eagle search algorithm

1 Introduction

Various factors often affect images, such as defects in recording devices, transmission media, and imaging systems [1,2]. These images exhibit low brightness, weakened detail, and poor contrast, all of which significantly impact the efficiency of computer vision systems [3,4]. Incomplete processing methods may lead to image degradation, while image enhancement techniques are essential to image processing. Their primary goal is to enhance the appearance of low-quality images and improve visual effects [5,6].

Image enhancement is important in many real-world applications, including medical image processing, satellite image analysis, remote sensing, and video processing [7,8]. It improves the visual quality of an image by expanding its intensity range. The region of interest can be easily observed in an image with good contrast. The key challenge in improving image quality is to maintain the essential features and brightness of images while performing contrast enhancement operations [9,10].

Image enhancement techniques are mainly divided into the following categories: i) Histogram equalization (HE) methods [11]. These methods improve contrast, and they are fast to process. However, they



can easily cause over-enhancement and loss of details due to grayscale merging. ii) Retinex methods [12,13]. The most classic methods include the single scale Retinex (SSR) algorithm, the multi-scale Retinex (MSR) algorithm, and the MSR with color restoration (MSRCR) algorithm. SSR uses Gaussian filtering for estimation, while MSR can be seen as a linear combination of multiple SSRs at different scales. MSR improves contrast and brightness, but it results in lower edge sharpness and some color distortion. MSRCR introduces color restoration to MSR to prevent distortion, but the colors may deviate from the original ones. Due to its excellent performance in enhancing contrast, brightness, and details, Retinex has been widely used in recent years. Therefore, the algorithm proposed in this paper is based on the Retinex technique.

Metaheuristic algorithms are utilized to solve complex problems by simulating optimization processes observed in nature [14–16]. These algorithms typically find near-optimal solutions across a wide range of potential solution spaces, and they have global search capabilities. In image enhancement, metaheuristic algorithms are widely used to optimize parameters such as brightness, contrast, and color balance. For instance, genetic algorithm (GA) [17], particle swarm optimization (PSO) [18,19], and bat algorithm (BA) [20] can effectively adjust the parameters of image enhancement techniques to improve visual quality. These algorithms enhance image quality by improving details and overall appearance.

It is not easy to enhance color images because it requires a large number of evaluations of an objective function that measures the quality of the enhanced image. To overcome limitations in current metaheuristic algorithms, such as their tendency to get trapped in local optima, slow convergence, and insufficient optimization of essential parameters for high-quality image enhancement, we propose an advanced bald eagle search (ABES) algorithm based on population learning, position updates, and control parameters. This algorithm allows for better exploration and exploitation within the solution space. ABES optimizes key parameters in gamma correction and Retinex to address color cast and enhance edge detail. It enhances prominent features and contrast more effectively while preserving the natural appearance of images. The primary contributions of this study are as follows:

1. The proposed image enhancement model is adaptable to a wide range of image types and it is not limited to any specific application. ABES incorporates an innovative position update mechanism, skillfully balancing global exploration with local search to enhance convergence speed over the original BES algorithm. This approach enables ABES to refine image details effectively and produces enhanced brightness and contrast consistency across various types of images.

2. ABES has been shown to be superior to other methods in terms of information entropy, peak signal-to-noise ratio (PSNR), structural similarity index (SSIM), and patch-based contrast quality index (PCQI) according to experimental results. The image quality has been improved both quantitatively and qualitatively, and ABES successfully enhances image details.

The main structure of this paper is as follows: [Section 2](#) introduces the latest research on color image enhancement, and [Section 3](#) presents the improved BES algorithm for image enhancement. [Section 4](#) discusses the experiments and statistical analysis conducted on multiple images, and [Section 5](#) provides a summary and perspective on the work presented in this paper.

2 Related Works

Image enhancement algorithms enable images to have more vivid colors and higher detail clarity. In this section, we will briefly introduce the latest research progress in image enhancement.

Zhang et al. considered image enhancement as an optimization problem and utilized the PSO algorithm to acquire the optimal solution [21]. Individual, local, and global optimizations adjust the flight direction of particles in PSO. The three channels of R, G, and B in color images are represented by quaternion

matrices, and the transformation parameters are optimized using an improved PSO. The flower pollination algorithm (FPA) is a well-known metaheuristic algorithm, but its operators may lead to false optimal positions on multi-modal surfaces. Das et al. enhanced FPA using fitness-based dynamic inertia weight and two popular differential evolution (DE) mutation techniques [22]. The modified FPA (PMFPA) balances evolutionary stages and locates the optimal values. It has been applied in image enhancement to measure its efficiency. Prakash et al. used an improved measurement method to enhance low-contrast images [23]. Chaotic mapping is incorporated into the crow search method to improve global optimization. Krill herd optimization is used to fine-tune the parameters in the new fitness function. Multi-scale Retinex is one of the most popular image enhancement methods. The control parameters, including Gaussian kernel size, gain, and offset, must be adjusted carefully based on the image content. Matin et al. introduced a multi-objective PSO method to optimize these parameters [24]. This method iteratively validates the visual quality of the enhanced image in terms of brightness, contrast, and color.

Low illumination in deep water often leads to poor clarity and low contrast in underwater images. The inherent wavelength absorption characteristics of water cause underwater images to have a blue-green tint. Therefore, it is a challenging task to study them. Sethi et al. proposed a method that uses multi-objective PSO (MOPSO) to adjust the contrast and information content of underwater images [25]. The objective functions of MOPSO correct color and contrast without introducing artifacts. The enhanced images contain more information and contrast. In coal mines, poor lighting conditions and high dust suspension lead to images with uneven lighting and low differentiation of facial features. Dai et al. proposed an improved image enhancement method [26]. Median filtering is selected for noise reduction based on the characteristics of coal mine images. Then, a gamma function and a fractional-order operator are introduced, and a PSO algorithm is proposed for image enhancement. Liu et al. introduced a hybrid image enhancement algorithm based on Retinex to improve the quality of drone images [27]. The algorithm uses a two-stage evolutionary computation to adjust the hyperparameters of the MSRRCR model automatically. The Rao-2 algorithm is employed for global search, and solutions are obtained by maximizing the objective function. The Nelder-Mead simplex method is used to refine the solutions through local search. The algorithm's performance is validated using real, low-quality drone images. Sathananthavathi et al. enhanced retinal fundus images with uneven illumination by adjusting brightness and contrast using PSO [28]. The proposed technique incorporates gamma correction in the Hue Saturation Value (HSV) color space and contrast adjustment in the Lab Color Space (LAB) color space. The PSO algorithm enhances manual and automatic image analysis systems by optimizing the contrast.

In the aforementioned studies, such as PSO and FPA, image enhancement capabilities have significantly improved in different fields. These algorithms excel at optimizing image brightness, contrast, and color correction, which are essential for improving visual quality. However, they also have some drawbacks. Although they are flexible and capable of adapting to specific challenges, these methods often involve increased computational complexity. For example, MOPSO may require significant computational resources, particularly when optimizing multiple parameters simultaneously. These algorithms can be prone to overfitting, especially when applied to highly specific image types, and they face difficulty in generalizing to other domains. Additionally, the parameters of these algorithms are highly dependent on the image features, and they require extensive manual intervention or experimentation to achieve optimal results. Recent works suggest that gamma correction and Retinex are essential for image enhancement. BES, as a new metaheuristic algorithm, has strong global search capabilities. However, there are still few reports on its application in image enhancement. In this study, we employ BES, gamma correction, and Retinex to enhance color images.

3 Proposed Image Enhancement Model

This study first applies gamma correction to images to address the phenomenon of color deviation. Then, the Retinex algorithm is used to adjust the hue of images to produce enhanced images. The parameters in gamma correction and Retinex significantly impact the quality of the enhanced images, so we optimize the key parameters using the BES algorithm. The image enhancement process is depicted in Fig. 1.

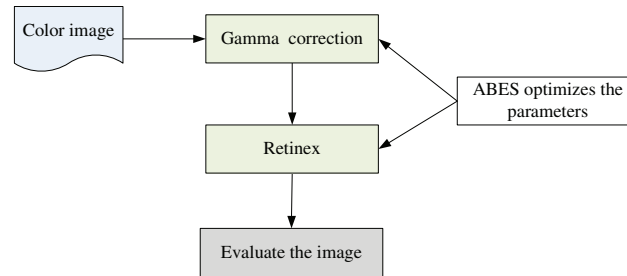


Figure 1: The image enhancement process

3.1 Objective Function

3.1.1 Gamma Correction

Gamma correction is a nonlinear operation used to encode and decode luminance or color values in images [29]. It adjusts the brightness and contrast of an image to achieve a more natural-looking result. The pixel values of an image are transformed using the following equations:

$$I_r(x) = I_r(x)^\alpha \quad (1)$$

$$I_g(x) = I_g(x)^\beta \quad (2)$$

$$I_b(x) = I_b(x)^\gamma \quad (3)$$

where I_r , I_g , and I_b represent the pixel values of the red, green, and blue channels, respectively. The parameters α , β , and γ control the brightness and contrast of an image. As these parameters increase, the contrast in the darker areas of an image diminishes, resulting in a darker appearance. Conversely, when these parameters decrease, the contrast in the brighter areas drops, causing the image to appear more colorful. These parameters are very important for image enhancement, but it isn't easy to accurately set them.

3.1.2 Retinex

Retinex is a widely used image enhancement approach based on the theory that an object's color is determined by its ability to reflect light at different wavelengths [30]. Retinex balances dynamic range compression, edge enhancement, and color consistency. It is computed as follows:

1. Input the original image $I(x, y)$.

2. Construct a Gaussian surround function $G(x, y) = Ke^{-\frac{x^2+y^2}{2\sigma^2}}$, where σ is the scale parameter, and K is a normalization constant, ensuring $\int \int G(x, y) dx dy = 1$.

3. Apply the Gaussian surround filter separately to the R, G, and B channels to get the illumination component: $L(x, y) = I(x, y) * G(x, y)$.

4. Take the logarithm and subtract the illumination component from the original image: $\log R(x, y) = \log I(x, y) - \log L(x, y)$.

5. Perform an exponential transformation $R'(x, y) = e^{\log R(x, y)}$. In practice, Retinex calculates the maximum (Max) and minimum (Min) values of $\log R(x, y)$, and then linearly scales each value: $R(x, y) = \frac{Value - Min}{Max - Min} \times 255$.

6. Output the reflectance component as the final enhanced image.

σ directly influences the algorithm's performance by controlling the scale of illumination estimation. However, it is usually set simply between [80, 120], which impacts the algorithm's enhancement effectiveness.

3.1.3 Objective Function

The amount of information or complexity in an image is measured by information entropy. For a grayscale image with L grayscale levels, entropy is defined as follows:

$$P(x_i) = \frac{\text{Number of pixels with value } i}{\text{Total number of pixels in an image}} \quad (4)$$

$$H_-(X) = - \sum_{i=1}^L P(x_i) \log_2 P(x_i) \quad (5)$$

where $H_-(X)$ represents the entropy of the pixel X . So the information entropy of color images is defined as follows:

$$H(X) = \frac{\sum_{i=1}^3 H_-(X)}{3} \quad (6)$$

where $H(X)$ represents the average entropy of the three channels in a color image.

The higher the information entropy, the greater the complexity and information content in an image. When the entropy is zero, it means that the image is completely uniform, and all pixel values are the same.

This study uses information entropy as an objective function. The value ranges of the six core parameters are as follows: α, β , and $\gamma \in [0.8, 2.2]$, $\sigma_1 \in [2, 50]$, $\sigma_2 \in [51, 100]$, and $\sigma_3 \in [101, 255]$, where σ_1, σ_2 , and σ_3 are three Gaussian kernels.

3.2 Advanced Bald Eagle Search Algorithm

BES mimics the hunting strategies and intelligent social behaviors of bald eagles when fishing [31,32]. BES consists of three stages during the predation process. In the selection stage, bald eagles choose a space with the most prey to search. Then, in the search stage, the eagles move within the selected space to hunt for prey. Finally, in the swooping stage, they move from the optimal position determined during the search stage.

In BES, individuals learn from anyone to enhance search capability but reduce the algorithm's convergence speed. We propose a new learning method to improve the balance between global and local searches of the BES algorithm. The population is evenly divided into three parts (P1, P2, and P3) based on the objective function values. P1 and P3 consist of the best and worst individuals, respectively, and P2 consists of the rest. In the proposed ABES algorithm, only the individuals in P3 update their positions, while those in P1 and P2 are responsible for guiding P3 to search. Algorithm 1 describes the pseudocode of ABES.

Algorithm 1: ABES

```

1 Initialize the population size  $N$ , the number of evaluations  $fs$ ;
2 Initialize the population  $pop$ ;
3  $nt = 0$ ;
4 Execute the objective function and save the values to  $cost$ ;
5  $nt = nt + N$ ;
6  $[, index] = sort(cost)$ ;
7 Acquire the global optimal solution;
8  $P1 = pop(index(1:N/3),:)$ ;
9  $P2 = pop(index(N/3+1:2*N/3),:)$ ;
10  $P3 = pop(index(2*N/3+1: N),:)$ ;
11 While  $nt \leq fs$  do
12     % the selection stage
13     Update the positions of P3 with Eq. (7);
14     Execute the objective function for P3;
15      $nt = nt + N/3$ ;
16     Update  $cost$ ;
17      $[, index] = sort(cost)$ ;
18      $P1 = pop(index(1:N/3),:)$ ;
19      $P2 = pop(index(N/3+1:2*N/3),:)$ ;
20      $P3 = pop(index(2*N/3+1: N),:)$ ;
21     % the search stage
22     Update the positions of P3 with Eq. (8);
23     Execute the objective function for P3;
24      $nt = nt + N/3$ ;
25     Update  $cost$ ;
26      $[, index] = sort(cost)$ ;
27     Acquire the global optimal solution;
28      $P1 = pop(index(1:N/3),:)$ ;
29      $P2 = pop(index(N/3+1:2*N/3),:)$ ;
30      $P3 = pop(index(2*N/3+1: N),:)$ ;
31     % the swooping stage
32      $P4 = [pop(1:3,:), mean(pop(1:3,:))]$ ;
33     Update the positions of P3 with Eq. (11);
34     Execute the objective function for P3;
35     Update  $cost$ ;
36      $nt = nt + N/3$ ;
37      $[, index] = sort(cost)$ ;
38     Acquire the global optimal solution;
39      $P1 = pop(index(1:N/3),:)$ ;
40      $P2 = pop(index(N/3+1:2*N/3),:)$ ;
41      $P3 = pop(index(2*N/3+1: N),:)$ ;
42 end
43 Output the global optimal solution;

```

3.2.1 Selection Stage

P1 guides the search of P3. In ABES, multiple optimal solutions participate in the population search, so they significantly improve the global search ability and robustness of the algorithm. This approach enhances population diversity and effectively prevents premature convergence. Furthermore, it provides various near-optimal solutions in complicated search spaces of image enhancement and keeps a balance between exploration and exploitation. ABES flexibly adjusts the search direction and improves the final solution quality and global optimization capability.

$$X_i(t + 1) = X_{best}(t) + 2 * rand(). * (X_p(t) - X_i(t)) \tag{7}$$

where $X_i(t)$ means the position of i at the t -th iteration. X_{best} presents the global optimal solution, and X_p is a random solution from P1.

3.2.2 Search Stage

P1 and P2 guide the search process of P3. In ABES, optimal and sub-optimal solutions collaboratively participate in the population search to improve the algorithm's global exploration ability and search efficiency. Optimal solutions direct the population toward high-quality regions and the algorithm converges rapidly on excellent solutions. Sub-optimal solutions assist in maintaining population diversity and extending the search range to explore potentially better solutions. This method achieves a balance between exploration and exploitation in complex and multi-modal search spaces and prevents the algorithm from prematurely converging on local optima.

$$X_i(t + 1) = X_i(t) + y_i * (X_i(t) - X_p(t)) + w_i * (X_i(t) - X_r(t)) \tag{8}$$

$$y = \frac{(a * \pi * rand(N) + R * rand(N)) * sin(a * \pi * rand(N))}{max(|(a * \pi * rand(N) + R * rand(N)) * sin(a * \pi * rand(N))|)} \tag{9}$$

$$w = \frac{(a * \pi * rand(N) + R * rand(N)) * cos(a * \pi * rand(N))}{max(|(a * \pi * rand(N) + R * rand(N)) * cos(a * \pi * rand(N))|)} \tag{10}$$

where N is the population size, and a and R are two coefficients. X_r is a random solution from P2.

3.2.3 Swooping Stage

To guide the search for P3, we utilize four global optimal solutions and their average position (P4), which is inspired by the EO algorithm [33]. They can enhance the algorithm's global search ability and convergence speed. The optimal solutions guide the population toward the potential areas, while the average position reduces the risk of over-convergence on a single solution.

$$X_i(t + 1) = rand() * X_{best}(t) + v_i * (X_i(t) - 2 * X_o(t)) + q_i * (X_i(t) - 2 * X_{best}(t)) \tag{11}$$

$$th = a * \pi * exp(rand(N)) \tag{12}$$

$$v = \frac{th * sinh(th)}{max(|th * sinh(th)|)} \tag{13}$$

$$q = \frac{th * cosh(th)}{max(|th * cosh(th)|)} \tag{14}$$

where X_o is a random solution from P4.

3.2.4 Analysis of the Values of th

In the swooping stage, the position update is influenced by th . According to Eq. (12), its value range is between $[10 * \pi, 10 * e * \pi]$. Fig. 2 shows the \sinh and \cosh functions within this range. The appearance of a curve is due to the overlap of these two functions. It can be concluded that the values of parameters ν and q are the same, and they lead to the same impact of P4 and the global optimal solution on individuals in Eq. (11), which reduces the algorithm's diversity. To address this issue, we randomly generate th each time ν and q are generated, as depicted in Eqs. (15) and (16).

$$\nu = \frac{a * \pi * \exp(\text{rand}(N)) * \sinh(a * \pi * \exp(\text{rand}(N)))}{\max(|a * \pi * \exp(\text{rand}(N)) * \sinh(a * \pi * \exp(\text{rand}(N)))|)} \quad (15)$$

$$q = \frac{a * \pi * \exp(\text{rand}(N)) * \cosh(a * \pi * \exp(\text{rand}(N)))}{\max(|a * \pi * \exp(\text{rand}(N)) * \cosh(a * \pi * \exp(\text{rand}(N)))|)} \quad (16)$$

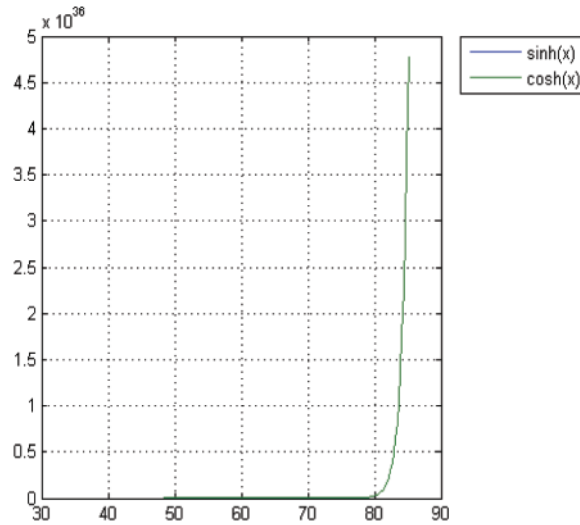


Figure 2: The values of th

3.2.5 Computational Complexity

The ABES algorithm primarily consists of position updates and objective function evaluations, which results in a time complexity of $O(fs * dim + fs * \log(N/3))$ and $O(fs * g)$, respectively. fs means the number of evaluations, g represents the execution time of the objective function, and N denotes the population size. Therefore, the overall maximum time complexity of the AEO algorithm is $O(fs * dim + fs * \log(N/3) + fs * g)$.

4 Experimental Results and Analysis

We compare the proposed algorithm with the original BES algorithm and three other recent image enhancement algorithms: PSO [21], chimp optimization algorithm (ChOA) [34], and PMFPA [22]. The population size for the algorithms is set to 30, and the maximum number of evaluations is 3000. Table 1 displays the main parameter configurations. We randomly select ten images from the benchmark datasets [35,36] as test images, as shown in Fig. 3.

Table 1: The main configurations of the compared algorithms

Algorithm	Key parameters
ChOA	$G1 = G2 = 1.95; G3 = G4 = 2.5;$
PSO	$c1 = 2; c2 = 2; V_{max} = 6; w_{max} = 0.9; w_{min} = 0.2;$
PMFPA	$p = 0.5;$
BES & ABES	$lm = 2; a = 10; R = 1.5;$



Figure 3: The test images

4.1 Experimental Analysis

Table 2 presents the average values of the objective function obtained by the algorithms. Among these, the ABES algorithm stands out, consistently outperforming ChOA, PSO, PMFPA, and BES in Img2, Img3, Img5, Img6, Img7, Img9, and Img10. ABES is particularly effective in optimizing the enhancement process across multiple images, and it is robust and adaptable when handling different image characteristics. In contrast, BES and PSO also demonstrate strong performance in 2 and 1 images, respectively. PMFPA falls behind, and it has the poorest image enhancement performance. The data reveals that the algorithms achieve the highest objective function value in Img5, which is notable for its rich details, diverse color distribution, and high contrast. Conversely, Img7 shows a uniform color distribution and fewer detail changes, so the algorithms receive the lowest objective function value. Overall, these findings underscore the significant differences in performance between ABES and the comparison algorithms. ABES performs less effectively than BES in Img1 and Img8, but it outperforms BES in the remaining eight images. ABES successfully improves image quality, and the modifications of ABES have positively impacted its overall effectiveness in image processing tasks.

Table 2: The object function values of the algorithms

Image	ChOA	PSO	PMFPA	BES	ABES
Img1	6.9313208	6.9313095	6.9309973	6.9314881	6.9314770
Img2	6.7784891	6.7784892	6.7784889	6.7784891	6.7784904
Img3	6.4391635	6.4391155	6.4391875	6.4391875	6.4391876
Img4	6.4590452	6.4590457	6.4590417	6.4590447	6.4590452
Img5	7.1397678	7.1397128	7.1397706	7.1397630	7.1398275
Img6	6.4134771	6.4134580	6.4134659	6.4134877	6.4135075
Img7	2.8151249	2.8151431	2.8150839	2.8151448	2.8151477
Img8	5.9185526	5.9184551	5.9184577	5.9186020	5.9185982
Img9	6.3087092	6.3087188	6.3086964	6.3087114	6.3087198
Img10	6.9671808	6.9671794	6.9671693	6.9671806	6.9671825

The Wilcoxon rank sum test is employed to assess the similarity of data among the algorithms due to the inherent randomness of metaheuristic algorithms and the closely clustered experimental results, as shown in Table 3. ‘-’ indicates optimal solutions, and ‘=’ and ‘-’ represents approximate and less than optimal solutions. This test reveals that the algorithms demonstrate consistent performance in Img3 and Img7. Notably, PSO and ABES show similar statistical data in several images, including Img3, Img4, Img7, Img9, and Img10. Furthermore, ABES and BES yield comparable experimental outcomes in Img3, Img7, Img9, and Img10. ChOA, PSO, PMFPA, BES, and ABES have the best performance in 3, 5, 2, 6, and 8 images, respectively.

Table 4 presents a detailed comparison of the computation times for five different algorithms applied to the benchmark images. From the table, it is clear that the proposed ABES algorithm takes more time to execute than the BES algorithm. This increase in computation time can be attributed to the enhanced strategies we incorporated into the BES framework, which aims to optimize performance further. Despite this longer processing time, ABES demonstrates significantly better effectiveness compared to PSO and PMFPA. Specifically, ABES requires approximately 6% to 14% more time than the fastest algorithm (BES), so it remains within an acceptable range for practical applications. This slight trade-off in computation time is justified

by the improved results in image quality that ABES delivers, so it is a worthwhile choice for prioritizing performance over speed in image enhancement.

Table 3: The Wilcoxon rank sum test of the algorithms

Image	ChOA	PSO	PMFPA	BES	ABES
Img1	<	<	<	–	<
Img2	<	<	<	<	–
Img3	=	=	=	=	–
Img4	<	–	<	<	=
Img5	<	<	<	<	–
Img6	<	<	<	<	–
Img7	=	=	=	=	–
Img8	<	<	<	–	<
Img9	<	=	<	=	–
Img10	=	=	<	=	–

Table 4: The average running time of the algorithms (Second)

Image	ChOA	PSO	PMFPA	BES	ABES
Img1	1866.4474308	1903.7601380	1916.6972753	1736.4951340	1946.1498832
Img2	5029.5122480	5146.1557750	5144.9533972	4576.2317771	5097.4275717
Img3	4992.8008616	5237.4601179	5128.7142667	4625.3296323	5115.6128347
Img4	6481.3384413	6459.2923668	6541.1921230	5889.0529270	6443.5308342
Img5	1499.7232139	1548.1359855	1574.3550040	1376.6786524	1492.5483674
Img6	2477.3369621	2533.1211209	2476.4649403	2248.6171799	2422.4248252
Img7	2185.2073501	2251.6667889	2179.5683065	2005.3000179	2298.6552435
Img8	2195.2893433	2448.7687880	2383.0096787	1973.2853856	2229.5729656
Img9	2313.6848186	2391.9349373	2395.2945390	2153.8249795	2328.8158131
Img10	2363.2564788	2463.9348643	2469.5228774	2244.6467335	2381.1878387

By improving population learning, position update, and control parameters in the BES algorithm, ABES effectively balances exploration and exploitation. The algorithm fine-tunes the key parameters of gamma correction and Retinex to achieve superior image enhancement results. They are critical for controlling brightness, contrast, and color fidelity, especially in challenging lighting conditions or low-visibility images. By dynamically adjusting these parameters, ABES can better preserve image details and enhance visual quality. Additionally, ABES excels in its robust image structure and color information handling. The objective function in ABES is optimized to prioritize information entropy and ensures that the structural integrity and perceptual quality of the images are enhanced. Compared to ChOA, PSO, PMFPA, and BES, ABES produces more apparent, sharper, and consistent results.

4.2 Image Quality Analysis

The algorithms' performance is further validated with PSNR, SSIM, and PCQI. PSNR quantitatively evaluates the degree of image change by calculating the differences between each pixel of the original

and processed images. A higher PSNR indicates less noise interference and better image quality in image processing. Table 5 clearly shows that the quality of images has significantly improved after being processed by the metaheuristic algorithms, with the ABES algorithm standing out for its superior performance in image enhancement. ABES performs better in Img6-Img10 than in Img1-Img5, and it demonstrates strong adaptability when dealing with different levels of image complexity. Furthermore, ABES outperforms other comparison algorithms in Img2, Img3, Img8, and Img9, and it exhibits high stability and reliability in image processing. While ChOA and PSNR achieve excellent PSNR results in 2 and 4 images, respectively, ABES shows more excellent overall stability.

Table 5: The PSNR values of the algorithms

Image	ChOA	PSO	PMFPA	BES	ABES
Img1	9.3918142	9.3720433	9.3957096	9.3959188	9.3838143
Img2	10.6872203	10.6872211	10.6872185	10.6872119	10.6872212
Img3	14.0466240	14.0466240	14.0466240	14.0466240	14.0474260
Img4	12.2643151	12.2643160	12.2643151	12.2643148	12.2643143
Img5	14.0725460	14.0674727	14.0664681	14.0767969	14.0733683
Img6	25.5021196	25.5006838	25.5009926	25.5033078	25.5020583
Img7	27.4215791	27.4230672	27.4207334	27.4209367	27.4210585
Img8	23.2891802	23.2913151	23.2881264	23.2880990	23.2954840
Img9	25.1624661	25.1624368	25.1624600	25.1625016	25.1626558
Img10	28.2789785	28.2780548	28.2782187	28.2800405	28.2788401

SSIM is an image quality assessment method that aligns closely with human visual perception. Unlike PSNR, SSIM evaluates the similarity between two images by comparing their structural information, and it provides a more precise reflection of changes in perceived image quality. Table 6 displays the performance of the algorithms using the SSIM metric. The results show that ABES outperforms other algorithms in Img3, Img8, Img9, and Img10, particularly excelling compared to PMFPA and BES. In this experiment, ChOA, PSO, PMFPA, and BES achieve the highest SSIM values in 1, 2, 1, and 2 images, respectively. Meanwhile, ABES also demonstrates strong competitiveness in image enhancement. It achieves high similarity between enhanced and original images in Img3, Img6, Img7, and Img10 and significantly improves the fidelity of image details. Despite the fluctuation of ABES's performance in SSIM, it still provides superior results for most images compared to other algorithms.

PCQI is a non-reference image quality assessment method. It focuses on the contrast and local structural information of images and measures the visual quality by evaluating the contrast changes in different regions (patches). Table 7 displays their experimental statistical results. ChOA, PSO, PMFPA, BES, and ABES achieve the highest PCQI values in 0, 4, 2, 3, and 1 images, respectively. Although ABES's performance is not as good as that of other algorithms, it demonstrates excellent stability. It ranks second in Img1, Img4, Img6, Img8, and Img10. In contrast, PSO and BES are extremely unstable. PSO performs poorly in Img2, Img3, Img6, and Img10, while BES struggles in Img1, Img4, Img5, Img6, Img8, Img9, and Img10. ABES has the highest average ranking, followed by PSO, ChOA, BES, and PMFPA. The algorithms significantly enhance the contrast of local patches in Img1 and Img5, and they effectively improve the visibility of details and edges. However, the local contrast of Img3 is originally low.

Table 6: The SSIM values of the algorithms

Image	ChOA	PSO	PMFPA	BES	ABES
Img1	0.7668246	0.7671130	0.7664877	0.7664849	0.7668731
Img2	0.8414747	0.8414747	0.8414747	0.8414746	0.8414747
Img3	0.9119185	0.9119185	0.9119185	0.9119185	0.9119186
Img4	0.5795675	0.5795674	0.5795675	0.5795676	0.5795676
Img5	0.7384272	0.7383266	0.7382731	0.7388474	0.7386818
Img6	0.9461961	0.9461967	0.9461975	0.9461914	0.9461940
Img7	0.9802068	0.9802114	0.9802064	0.9802069	0.9802072
Img8	0.8233620	0.8233785	0.8233448	0.8233405	0.8234008
Img9	0.8954005	0.8953957	0.8954010	0.8954048	0.8954062
Img10	0.9755229	0.9755221	0.9755215	0.9755229	0.9755238

Table 7: The PCQI values of the algorithms

Image	ChOA	PSO	PMFPA	BES	ABES
Img1	1.0545133	1.0546331	1.0544268	1.0545527	1.0545603
Img2	0.6291967	0.6288665	0.6288663	0.6296597	0.6290641
Img3	0.3480011	0.3479490	0.3478296	0.3481972	0.3479764
Img4	0.9457725	0.9457727	0.9457720	0.9457724	0.9457726
Img5	1.0450764	1.0450854	1.0450618	1.0450552	1.0451124
Img6	0.9168141	0.9168083	0.9168192	0.9168149	0.9168179
Img7	0.5508667	0.5508714	0.5508549	0.5508738	0.5508712
Img8	0.7778889	0.7781890	0.7778776	0.7777906	0.7779986
Img9	0.8792422	0.8792468	0.8792399	0.8792388	0.8792409
Img10	0.9026974	0.9026900	0.9027192	0.9026936	0.9027087

ABES maintains a balance between exploration and exploitation. It reduces the risk of premature convergence, a common limitation of other algorithms. As a result, ABES can explore a broader range of potential solutions and produce higher-quality image enhancements. The objective function values and their Wilcoxon rank sum, running time, PSNR, SSIM, and PCQI demonstrate the high efficiency of ABES in color image enhancement.

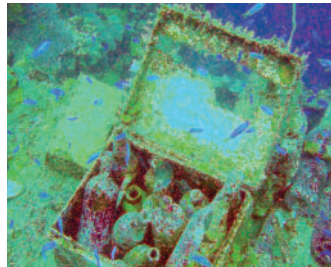
4.3 Evaluation of the Enhanced Images Visually

From Fig. 4, it can be observed that the images obtained by ABES show significant improvement compared to the original images. Img1–Img5 are underwater images where the original images suffer from severe color distortion. The enhanced images no longer exhibit these issues. In Img1, ABES clearly distinguishes the fish from the surrounding corals, and details such as the fish scales, eyes, and lips are more clearly portrayed. Although the objects in the enhanced Img2 appear somewhat blurry, they remain visually distinguishable from the surroundings. Img3 has been improved, while many details are still missing. The most noticeable improvements in Img4 are the clearer background and the more vivid appearance of the fish. The colors in Img5 are well restored, and the edges are more distinct and clear. ABES enhances the contrast in Img6–Img10, so they appear more realistic and vivid. The resulting image of Img6 effectively

handles the problem of different window reflections. Img7 contains a lot of red content. The processed image is unaffected by this color and enhances the stripes of the wooden slats. The sky in Img8 is gray, but the sky in the enhanced image is blue. The colors of the flowers in the processed Img9 are more vibrant, and the green of the leaves is intensified. Both the brightness and detail in Img10 have been significantly enhanced.



(a) Img1-ABES



(b) Img2-ABES



(c) Img3-ABES



(d) Img4-ABES



(e) Img5-ABES



(f) Img6-ABES



(g) Img7-ABES



(h) Img8-ABES



(i) Img9-ABES



(j) Img10-ABES

Figure 4: The enhanced images by ABES

5 Conclusions

This study presents an improved BES algorithm for the multi-stage process of image enhancement. By utilizing gamma correction and Retinex techniques, ABES significantly improves image quality and optimizes core parameters to bring out details, contrast, and clarity. Through rigorous benchmarking, ABES demonstrates superior performance over other metaheuristic algorithms in terms of key image quality metrics, including information entropy, PSNR, SSIM, and PCQI. According to simulation results, the proposed image enhancement method is less influenced by the original brightness of images and provides better contrast and clarity than the comparison image enhancement methods. Although the ABES algorithm improves image details and structural similarity, these benefits come at the cost of increased runtime. They may limit its scalability and applicability to applications where speed and simplicity are critical.

In the future, the proposed image enhancement algorithm could be utilized to enhance low-light or high-noise images from challenging environments like deep-sea or satellite images. ABES is also employed to process large-scale and high-resolution images more efficiently in remote sensing and geospatial analysis. We intend to integrate advanced learning techniques, such as deep learning-assisted parameter optimization, to enable real-time adaptation to diverse image characteristics.

Acknowledgement: We are grateful to the reviewers and the editor for their assistance in finalizing this paper.

Funding Statement: This work is supported by the Research on the Key Technology of Damage Identification Method of Dam Concrete Structure based on Transformer Image Processing (242102521031), the project Research on Situational Awareness and Behavior Anomaly Prediction of Social Media Based on Multimodal Time Series Graph (232102520004), and Key Scientific Research Project of Higher Education Institutions in Henan Province (25B520019).

Author Contributions: The authors confirm contribution to the paper as follows: study conception and design: Pei Hu; methodology, Pei Hu; data collection: Yibo Han; analysis and interpretation of results: Yibo Han, Pei Hu; draft manuscript preparation: Jeng-Shyang Pan; manuscript final layout and preparation for submission: Pei Hu, Jeng-Shyang Pan. All authors reviewed the results and approved the final version of the manuscript.

Availability of Data and Materials: Data is contained within this study, further inquiries can be directed to the corresponding author.

Ethics Approval: This study did not involve any human or animal subjects, and therefore, ethical approval was not required.

Conflicts of Interest: The authors declare no conflicts of interest to report regarding the present study.

References

1. Gite S, Mishra A, Kotecha K. Enhanced lung image segmentation using deep learning. *Neural Comput Appl.* 2023;35(31):22 839–53. doi:10.1007/s00521-021-06719-8.
2. Agrawal A, Gopalakrishnan K, Choudhary A. Materials image informatics using deep learning. In: *Handbook on big data and machine learning in the physical sciences: volume 1. Big data methods in experimental materials discovery.* USA: World Scientific; 2020. p. 205–30.
3. Zhang Y, Liu X, Lv Y. A hybrid swarming algorithm for adaptive enhancement of low-illumination images. *Symmetry.* 2024;16(5):533. doi:10.3390/sym16050533.
4. Galvez A, Iglesias A, Osaba E, Del Ser J. Bat algorithm method for automatic determination of color and contrast of modified digital images. In: *2020 IEEE 44th Annual Computers, Software, and Applications Conference (COMPSAC); 2020; Madrid, Spain: IEEE.* p. 1195–200.

5. Madhavan MV, Thanh DNH, Khamparia A, Pande S, Malik R, Gupta D. Recognition and classification of pomegranate leaves diseases by image processing and machine learning techniques. *Comput Mater Contin.* 2021;66(3):2939–55. doi:10.32604/cmc.2021.012466.
6. Gupta R, Khari M, Gupta D, Crespo RG. Fingerprint image enhancement and reconstruction using the orientation and phase reconstruction. *Inf Sci.* 2020;530(7):201–18. doi:10.1016/j.ins.2020.01.031.
7. Munadi K, Muchtar K, Maulina N, Pradhan B. Image enhancement for tuberculosis detection using deep learning. *IEEE Access.* 2020;8:217897–907. doi:10.1109/ACCESS.2020.3041867.
8. Cheng J, Li H, Li D, Hua S, Sheng VS. A survey on image semantic segmentation using deep learning techniques. *Comput Mater Contin.* 2023;74(1):1941–57. doi:10.32604/cmc.2023.032757.
9. Jiang P, Xue Y, Neri F. Convolutional neural network pruning based on multi-objective feature map selection for image classification. *Appl Soft Comput.* 2023;139:110229. doi:10.1016/j.asoc.2023.110229.
10. Guo J, Wang H, Xue X, Li M, Ma Z. Real-time classification on oral ulcer images with residual network and image enhancement. *IET Image Process.* 2022;16(3):641–6. doi:10.1049/ipr2.12144.
11. Braik M. Hybrid enhanced whale optimization algorithm for contrast and detail enhancement of color images. *Cluster Comput.* 2024;27(1):231–67. doi:10.1007/s10586-022-03920-9.
12. Jalab HA, Al-Shamasneh AR, Shaiba H, Ibrahim RW, Baleanu D. Fractional Rényi entropy image enhancement for deep segmentation of kidney MRI. *Comput Mater Contin.* 2021;67(2):2061–75. doi:10.32604/cmc.2021.015170.
13. Shen WW, Chen L, Liu S, Zhang YD. An image enhancement algorithm of video surveillance scene based on deep learning. *IET Image Process.* 2022;16(3):681–90. doi:10.1049/ipr2.12286.
14. Xue X. Automatic knowledge graph matching via self-adaptive designed genetic programming. *Knowl Based Syst.* 2024;293:111628. doi:10.1016/j.knsys.2024.111628.
15. Cai Z, Yang X, Zhou MC, Zhan ZH, Gao S. Toward explicit control between exploration and exploitation in evolutionary algorithms: a case study of differential evolution. *Inf Sci.* 2023;649:119656. doi:10.1016/j.ins.2023.119656.
16. Pan JS, Hu P, Snášel V, Chu SC. A survey on binary metaheuristic algorithms and their engineering applications. *Artif Intell Rev.* 2023;56(7):6101–67. doi:10.1007/s10462-022-10328-9.
17. Acharya UK, Kumar S. Genetic algorithm based adaptive histogram equalization (gaahe) technique for medical image enhancement. *Optik.* 2021;230:166273. doi:10.1016/j.ijleo.2021.166273.
18. Kanmani M, Narsimhan V. An image contrast enhancement algorithm for grayscale images using particle swarm optimization. *Multimed Tools Appl.* 2018;77(18):23371–87. doi:10.1007/s11042-018-5650-0.
19. Hu P, Pan JS, Chu SC, Sun C. Multi-surrogate assisted binary particle swarm optimization algorithm and its application for feature selection. *Appl Soft Comput.* 2022;121:108736. doi:10.1016/j.asoc.2022.108736.
20. Dhal KG, Das S. A dynamically adapted and weighted bat algorithm in image enhancement domain. *Evol Syst.* 2019;10(2):129–47. doi:10.1007/s12530-018-9216-1.
21. Zhang X, Ren Y, Zhen G, Shan Y, Chu C. A color image contrast enhancement method based on improved PSO. *PLoS One.* 2023;18:e0274054. doi:10.1371/journal.pone.0274054.
22. Das A, Dhal KG, Ray S, Galvez J, Das S. Fitness based weighted flower pollination algorithm with mutation strategies for image enhancement. *Multimed Tools Appl.* 2022;81(20):28955–86. doi:10.1007/s11042-022-12879-z.
23. Prakash SJ, Chetty MSR, Jayalakshmi A. Contrast enhancement of images using meta-heuristic algorithm. *Traitement Signal.* 2021;38(5):1345–51. doi:10.18280/ts.380509.
24. Matin F, Jeong Y, Park H. Retinex-based image enhancement with particle swarm optimization and multi-objective function. *IEICE Trans Inf Syst.* 2020;103(12):2721–4. doi:10.1587/transinf.2020EDL8085.
25. Sethi R, Sreedevi I. Adaptive enhancement of underwater images using multi-objective PSO. *Multimed Tools Appl.* 2019;78(22):31823–45. doi:10.1007/s11042-019-07938-x.
26. Dai L, Qi P, Lu H, Liu X, Hua D, Guo X. Image enhancement method in underground coal mines based on an improved particle swarm optimization algorithm. *Appl Sci.* 2023;13(5):3254. doi:10.3390/app13053254.
27. Liu X, Wang Z, Wang L, Huang C, Luo X. A hybrid retinex-based algorithm for UAV- taken image enhancement. *IEICE Trans Inf Syst.* 2021;D(11):2024–7. doi:10.1587/transinf.2021EDL8050.

28. Sathananthavathi V, Indumathi G. Particle swarm optimization based retinal image enhancement. *Wirel Pers Commun.* 2021;121(3):1–13. doi:10.1007/s11277-021-08649-z.
29. Alhajlah M. Underwater image enhancement using customized CLAHE and adaptive color correction. *Comput Mater Contin.* 2023;74(3):5157–72. doi:10.32604/cmc.2023.033339.
30. Cai R, Chen Z. Brain-like retinex: a biologically plausible retinex algorithm for low light image enhancement. *Pattern Recognit.* 2023;136:109195. doi:10.1016/j.patcog.2022.109195.
31. Alsattar HA, Zaidan A, Zaidan B. Novel meta-heuristic bald eagle search optimisation algorithm. *Artif Intell Rev.* 2020;53(3):2237–64. doi:10.1007/s10462-019-09732-5.
32. Li W, Shi T, Wang L, Xie W. A bald eagle search optimization based weighted rank aggregation method for microarray data classification. In: *Proceedings of the 2023 15th International Conference on Bioinformatics and Biomedical Technology*; 2023; Belgrade, Serbia. p. 54–60.
33. Faramarzi A, Heidarinejad M, Stephens B, Mirjalili S. Equilibrium optimizer: a novel optimization algorithm. *Knowl Based Syst.* 2020;191:105190. doi:10.1016/j.knosys.2019.105190.
34. Du N, Luo Q, Du Y, Zhou Y. Color image enhancement: a metaheuristic chimp optimization algorithm. *Neural Process Lett.* 2022;54(6):4769–808. doi:10.1007/s11063-022-10832-7.
35. Paul A. Adaptive tri-plateau limit tri-histogram equalization algorithm for digital image enhancement. *Vis Comput.* 2023;39(1):297–318. doi:10.1007/s00371-021-02330-z.
36. Han G, Wang M, Zhu H, Lin C. UIEGAN: adversarial learning-based photorealistic image enhancement for intelligent underwater environment perception. *IEEE Trans Geosci Remote Sens.* 2023;61:1–14. doi:10.1109/TGRS.2023.3281741.